Impact of Persistence on the Age of Information in 5G NR-V2X Sidelink Communications

Alexey Rolich*, Ion Turcanu†, Alexey Vinel‡ , and Andrea Baiocchi*
*Dept. of Information Engineering, Electronics and Telecommunications (DIET), University of Rome Sapienza, Italy
†Luxembourg Institute of Science and Technology (LIST), Luxembourg
‡Karlsruhe Institute of Technology (KIT), Karlsruhe, Germany
alexey.rolich@uniroma1.it ion.turcanu@list.lu
alexey.vinel@kit.edu andrea.baiocchi@uniroma1.it

***Abstract*—Cooperative awareness and its evolution to collective perception is one of the key building blocks of the Intelligent Transportation Systems (ITS). Cooperative awareness is achieved by continuously exchanging update messages between neighboring nodes (vehicles, pedestrians, infrastructure) interacting on the road. A promising technology designed to support cooperative awareness is 5G NR-V2X, which enables sidelink communications through its Mode 2 operation mode. In Mode 2, vehicles can use Semi-Persistent Scheduling (SPS) to autonomously select and reserve resources to transmit successive messages. While the general performance of SPS has been studied recently, the impact of the persistence on the freshness of update messages has not been investigated. In this paper, we aim to answer the following question: is persistence beneficial in terms of the average Age of Information (AoI) metric? To this end, we define a simplified model of the SPS that lends itself to analytical evaluation and optimization. Comparison with simulations shows that the model is quite accurate and robust. Using this model, we obtain evidence for the existence of an optimal persistence level, which is not apparent when looking at other performance metrics, such as throughput or simply Peak AoI (PAoI). The optimal persistence probability emerges when looking at the system through the lens of average AoI.**

***Index Terms*—5G NR-V2X, Sidelink Communications, Age of Information, Semi-Persistent Scheduling, V2X Communications, Autonomous Resource Selection.**

I. INTRODUCTION

Vehicle-to-Everything (V2X) communication, which allows road users to exchange information with each other, the road infrastructure, the edge, and the cloud, is intended to help connected and automated (and in the future, autonomous) vehicles be aware of their driving environment [1]. From this perspective, V2X radio can be seen as a sensor that complements other on-board sensors, such as video cameras and radars, in cases where the latter are of limited use due to the lack of optical visibility between objects.

Recent progress in V2X standardization has shifted the attention of the community from *cooperative awareness*, where participants share their status information such as current position and speed [2], to *collective perception*, where sensor information about visible objects is shared with nearby users [3], and paved the way for *cooperative maneuvering*, where vehicles can announce and agree on their driving intentions [4]. In all three cases, the fundamental communication enabler is a continuous one-hop broadcast of periodic messages that provide real-time updates of a variety of time-sensitive information.

Two technologies have been considered for V2X – wireless local area network solutions, widely referred to as IEEE 802.11p (or ITS-G5), and cellular-based approaches, which originated from LTE and have evolved to the current state-of-the-art 5G New Radio (NR) [5]–[7]. While the former is a more-or-less well-understood, relatively lightweight Wi-Fi-based protocol, the latter is a more elaborate one – it is embedded in a complex architecture of a new generation broadband wireless access network, and is the subject of numerous ongoing research efforts.

Direct inter-vehicle communication without the need for base station coverage (Mode 2 sidelink) together with a Semi-Persistent Scheduling (SPS) mechanism is a promising approach to support periodic broadcasting in 5G NR, which is central to cooperative automated driving applications. In this paper, we conduct the performance evaluation of this approach with a focus on the persistence aspect. Briefly, each user can randomly select a transmission opportunity from a pool of available resources each time there is an update message to transmit, or it can keep the selected channel resource for a certain time window before randomly switching to another one. In the latter case, the persistence probability is introduced to characterize the frequency of such a switch. In both cases, some of the users may unluckily choose the same resource, resulting in a mutual interference and the inability of others to receive the updates. The key research question addressed in this work, the answer to which is not intuitively clear in this context, is whether or not this persistence is beneficial for performance. From classical multiple access theory, persistence can be seen as a form of reservation in a random access scheme [8].

In recent years, the performance evaluation of status broadcast updates in V2X is characterized not only by traditional communication network metrics such as throughput or mean delay. Instead, similar to other machine-to-machine communication systems, where the freshness of the update information is crucial, Age of Information (AoI) is proposed [9]. In the context of cooperative awareness and collective perception, AoI is the key performance metric that characterizes a vehicle's environmental sensing gains due to V2X communications [10]. For cooperative maneuvering, the AoI can be used in the formal safety evaluation of automated driving [11].

In this paper, we present a mathematical model to characterize the performance of the SPS in 5G NR-V2X from the perspective of AoI. Our goal is to understand whether there are optimal persistence choices or whether the performance is monotonic with respect to the persistence probability. The main contributions of this paper are:

- to understand the impact of persistence on the performance of one-hop update message broadcasts, specifically on AoI, with application to the evaluation of the SPS

21st Mediterranean Communication and Computer Networking Conference (MedComNet 2023)

Table I
LIST OF ACRONYMS

Acronym	Meaning
AoI	Age of Information
BSM	Basic Safety Message
CAM	Cooperative Awareness Message
CBR	Channel Busy Ratio
DS	Dynamic Scheduling
DTMC	Discrete Time Markov Chain
ITS	Intelligent Transportation Systems
NR	New Radio
PAoI	Peak AoI
PCR	Packet Collision Ratio
PDF	Probability Density Function
PDR	Packet Delivery Ratio
PIR	Packet Inter-Reception Delay
PRR	Packet Reception Ratio
RB	Resource Block
RC	Reselection Counter
RRI	Resource Reservation Interval
RSRP	Reference Signal Receive Power
SC	Sub-Channel
SCI	Sidelink Control Information
SPS	Semi-Persistent Scheduling
TB	Transport Block
UE	User Equipment
V2X	Vehicle-to-Everything

mechanism in 5G NR V2X, and
- to define an accurate analytical model to optimize the persistence probability.

The paper is organized as follows. Section II provides an overview of NR-V2X sidelink communications and analyzes the related works on the performance evaluation of SPS and AoI metric. Section III describes the proposed analytical and simulation models and the implementation details. Section IV validates the analytical model against simulations and discusses the obtained results. Section V concludes the paper. Table I lists the acronyms used in this paper.

II. BACKGROUND AND RELATED WORKS

5G NR-V2X sidelink technology has recently been introduced to enable advanced use cases that rely on cooperative perception and maneuvering [12]. Comprehensive overviews of 5G NR-V2X, describing its physical layer design and resource allocation mechanisms, as well as its two operation modes (Mode 1 and Mode 2), are provided in [13] and [14]. While Mode 1 relies on a centralized resource allocation mechanism, Mode 2 introduces two distributed allocation strategies – SPS and Dynamic Scheduling (DS) – that allow vehicles to select their transmission resources autonomously.

In this section, we first provide an overview of the resource allocation mechanism in NR-V2X Mode 2. We then analyze the related works that investigate the performance of the SPS mechanism in terms of the most common metrics. We finally describe the existing literature that analyzes the AoI metric in the context of 5G NR-V2X.

A. Overview of NR-V2X Mode 2

In NR-V2X, messages are transmitted in Transport Blocks (TBs). The communication resources allocated to TBs are called Sub-Channels (SCs). An SC consists of several Resource Blocks (RBs) belonging to the same time slot and occupying adjacent frequencies. An SC carries a control field called Sidelink Control Information (SCI) and a TB or part of a TB, if the latter is fragmented across multiple SCs.

There are two possible approaches to allocate resources for TB transmission in Mode 2 - DS and SPS [15]. In DS mode, resources are selected each time a new TB is generated. SPS, instead, selects resources for a number of consecutive Reselection Counter (RC) TBs.

The time period between consecutive TB transmissions is determined by the Resource Reservation Interval (RRI). Possible RRI values are {0, [1: 99], 100, 200, 300, 400, 500, 600, 700, 800, 900, 1000} ms. The RRI is selected for every new TB from a list of maximum 16 pre-configured values in the resource pool [16].

The RC value depends on the selected RRI and is randomly chosen every time a new resource must be selected. In particular, RC is randomly chosen within $[5, 15]$ when $\mathit{RRI} \geq 100\,\mathrm{ms}$. If $\mathit{RRI} < 100\,\mathrm{ms}$, then RC is randomly set within $[5\cdot C, 15\cdot C]$, where

$$C = \frac{100}{\max(20, \mathit{RRI})}. \tag{1}$$

RC is decremented by 1 with every TB transmission. When $\mathrm{RC} = 0$, a new resource is selected with probability $(1 - P)$, where $P \in [0, 0.8]$. Otherwise, the same resources with the same RRI will be used for a number of consecutive RC TBs, where RC is again randomly chosen according the rules described above.

A simplified example of the SPS resource selection process is shown in Figure 1. Each User Equipment (UE) has a *sensing window* (of $1100\,\mathrm{ms}$ or $100\,\mathrm{ms}$, depending on the configuration), used to determine which SCs are reserved by other UEs for their own TB transmissions. If the Reference Signal Receive Power (RSRP) of these transmissions exceeds a preconfigured threshold, they are excluded from the pool of candidate resources in the *selection window*. In particular, the SPS resource selection algorithm has two main steps [13]:

1) Exclude candidate resources (i.e., SCs) in the selection window corresponding to (i) reservations received from other UEs in the 1st-stage SCI detected during the sensing window; (ii) measurements of a received power level exceeding a given threshold for those SCs for which no explicit reservation could be verified. Other SCs are also excluded, corresponding to those that cannot be received and checked by the node during the sensing window due to half-duplex operations.
2) Randomly select the sidelink resource from the list of available candidate resources.

B. SPS Performance Evaluation

Several recent works have investigated the performance of cellular V2X sidelink communication. Gonzalez-Martín et al. [17] present the first analytical models to evaluate the performance of LTE-V2X Mode 4 [18], which defines the first version of SPS (later inherited and updated in NR-V2X Mode 2). The authors focus on the Packet Delivery Ratio (PDR) as well as different types of packet errors. Segata et al. [19] present a first analysis of the LTE-V2X Mode 4 performance and its impact on vehicle platooning applications. Their results highlight important limitations of this technology in supporting cooperative driving solutions, mainly due to the observed bursts of lost packets, even in lightly loaded scenarios.

The optimal configuration of parameters in LTE-V2X Mode 4 is studied in [20]. The authors evaluate the impact of the persistence probability P (i.e., the probability of keeping

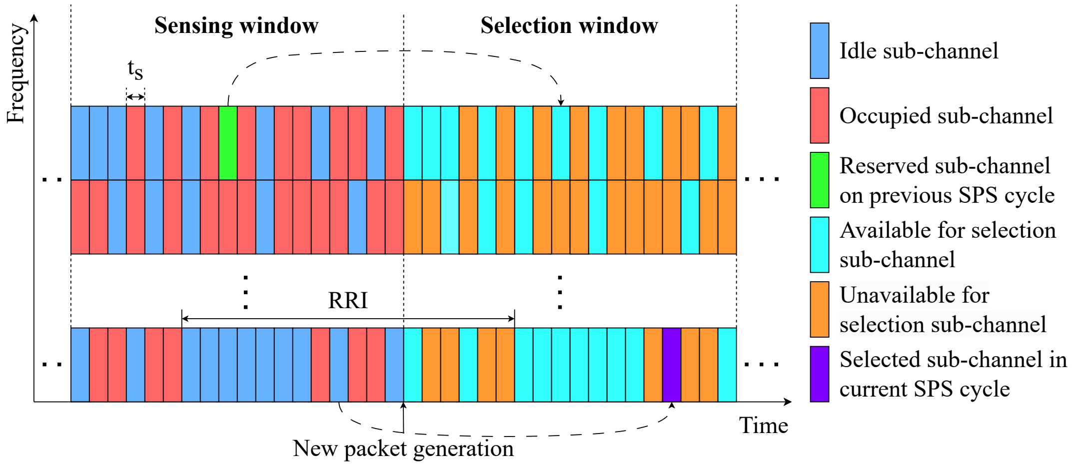

Figure 1. Simplified example of SPS-based scheduling in NR-V2X Mode 2.

the selected resource) on the PDR metric and conclude that increasing P does not always increase the PDR. The delay performance of SPS is analyzed in [21]. Here, the authors identify the main factors that affect the performance of SPS and propose optimizations of several configuration parameters, such as sensing range, transmit power, and resource reservation.

Bazzi et al. [22] propose an extension to the legacy SPS mechanism in LTE-V2X Mode 4 in order to handle wireless blind spot situations, i.e., successive packet losses due to wrong sidelink resource allocation. The performance of the proposed extended mechanism – in terms of Packet Reception Ratio (PRR) – is evaluated using a discrete-event network simulator and compared with the legacy SPS approach. Wu et al. [23] propose to replace SPS with another distributed channel access protocol for LTE-V2X Mode 4 designed to alleviate the half-duplex issue and the packet collision problem in SPS. They propose a self-adaptive scheduling protocol able to schedule RBs in the two-hop neighbor set and avoid merging collisions dynamically. The proposed solution is shown to perform better in terms of PDR and throughput compared to other legacy mechanisms.

The coexistence of periodic and aperiodic traffic in LTE-V2X Mode 4 is investigated in [24]. Here, the authors propose a standard-compliant resource reservation mechanism to handle aperiodic traffic and define an analytical model that determines the throughput of the proposed solution. This solution is compared to the standard SPS in terms of PRR, Packet Inter-Reception Delay (PIR), and Channel Busy Ratio (CBR). Bartoletti et al. [25] analyze the impact of the mismatch between the packet generation and resource allocation on the system performance. The authors provide a case study based on Cooperative Awareness Message (CAM) generation according to ETSI specifications and show that PRR performance can be improved if resources are reserved more frequently than needed.

Jeon et al. [26] show that message collisions in LTE-V2X Mode 4 can be reduced by reducing the uncertainties in the resources to be used for the next sequence of messages. They propose to piggyback the "lookahead" information on the periodic safety messages in order to learn the next starting resource location in the time-frequency plane. However, implementation of this approach requires the inclusion of the lookahead information into the control part of the packet, resulting in higher overhead. Haider and Hwang [27] take a different approach and propose to adapt the transmit power instead in order to improve the performance of LTE-V2X Mode 4. In particular, they propose a power control mechanism for CAM transmissions and demonstrate its benefits in high density scenarios.

Todisco et al. [28] analyze the performance of NR-V2X Mode 2 with periodic traffic, focusing on the use of flexible NR numerology and modifications to the SPS, covering different procedures and settings for candidate resource discovery and allocation. The results of this study suggest that the persistent reservation of resources must be tailored to the actual traffic generation patterns. The performance of NR-V2X Mode 2 with aperiodic traffic and variable packet sizes is evaluated in [29], focusing on the analysis of PDR and Packet Collision Ratio (PCR). The results of this study suggest that further improvements to the MAC of NR-V2X are needed in order to efficiently support aperiodic traffic.

C. AoI in 5G NR-V2X

The studies described in Section II-B provide valuable insight into the performance of SPS. However, none of these works analyze the AoI [30], which is a critical performance metric that measures the freshness of cooperative awareness and perception message updates. Although it has been extensively studied in the context of IEEE 802.11-based vehicular communications [10], [31]–[33], there are only few existing works that analyze the AoI performance in 5G NR-V2X.

Peng et al. [34] are the first to adopt and optimize the AoI metric in cellular sidelink communications. They propose a new resource allocation mechanism that utilizes piggyback feedback to avoid collision errors. They find the optimal RRI for a given number of vehicles and propose a method to adjust the RRI in real time. However, the proposed solution does not perform well when aperiodic traffic needs to be transmitted.

A similar idea is proposed in [35], where the authors propose an improved adaptive SPS that allows each vehicle to dynamically adjust the RRI in real time. The proposed mechanism outperforms SPS both in terms of traffic safety and network performance. This work also proposes an AoI-aware RRI selection algorithm that measures the AoI values of neighboring vehicles to select an age-optimal RRI.

Fouda et al. [36] study the possibility of reducing the probability of persistent Basic Safety Message (BSM) collisions by randomly skipping SPS reserved resources. They combine the concept of one-shot transmissions with SPS in order to improve the AoI tail of BSM transmissions and demonstrate the performance improvement over traditional SPS.

Cao et al. [37] analyze the parameters of the SPS mechanism proposed in NR-V2X Mode 2 from an AoI perspective in order to investigate the freshness of BSMs. The authors present an analytical model that shows that the expected Peak AoI (PAoI) performance is mainly influenced by the RRI parameter. However, the AoI metric is not considered as a possible parameter of the SPS mechanism. The impact of the radio resource keeping probability on AoI is also not investigated. The authors conclude that the number of successful transmissions is not sensitive to changes in radio resource persistence probability.

In this paper, we investigate the performance of 5G NR-V2X SPS mechanism from a different perspective. Specifically, we focus on the impact of the persistence probability P, i.e., the probability of keeping the same resources for the next packet transmissions, on the freshness (i.e., AoI) of cooperative awareness updates.

III. System Model

A. Model Assumptions and Notation

Consider a set of N nodes sharing a 5G NR-V2X communication channel used according to Mode 2 [37]. We want to answer the following question: is persistence beneficial for cooperative awareness, and to what extent? To gain a full understanding on this point, we resort to a simplified model that retains the essential characteristics of the SPS algorithm.

We make the following assumptions:

1) Nodes hear each other (no hidden nodes).
2) All nodes use the same RRI.
3) The sensing window used by a node to identify candidate SCs extends over exactly one RRI.
4) Only broadcast traffic is considered, so no ACK is provided and no retransmission is scheduled.
5) Nodes generate a new message for each RRI.
6) The SC is sized to carry one complete message, i.e., one TB plus its associated SCI (both first and second stage) fit into one SC.
7) The RC is drawn from a Geometric probability distribution, i.e., $\mathcal{P}(RC = j) = c^{j-1}(1 - c)$, for $j \geq 1$. Note that the mean RC is equal to $\overline{RC} = 1/(1-c) \geq 1$, hence c can be identified as $c = 1 - 1/\overline{RC}$.
8) The number of nodes N is less than the number K of SCs available in one RRI.

Assumptions 5 and 6 correspond to the best situation for the SPS algorithm, since message generation is exactly periodic and each new message fits exactly into the reserved resource. It is known that SPS can lead to wasted resources and inefficiency in the case of random new message generation and variable message sizes [37]. In this analysis, we assume the best possible configuration for SPS, since our goal is to understand the impact of persistence on performance and to optimize system configuration in a context where the persistent approach of this algorithm makes sense. Note also that as a consequence of Assumption 8, there is always at least one idle SC in each RRI. Assumption 3 is actually implied by the fact that nodes generate new messages periodically, provided that the selection window is not smaller than the common value of the RRI of all nodes.

Table II
Main notation used in the paper

Symbol	Meaning
N	Number of nodes.
K	Number of SCs per allocation period.
P	Persistence probability.
c	Parameter of the Geometric distribution of the RC; it is $\overline{RC} = 1/(1-c)$, where $\overline{RC}$ denotes the mean RC value.
q	Probability to change the SC in the next RRI with respect to the currently used one. It is $q = (1-P)(1-c)$.
$X_i(t)$	State of SC i in the t-th RRI, defined as the number of nodes that are currently using SC i to transmit their messages; it is $X_i(t) \in \{0, 1, \dots, N\} (i = 1, \dots, K)$.
$S_j(t)$	State of node j in the t-th RRI, defined as 1 if node j transmits its message with success in that RRI, 0 otherwise $(j = 1, \dots, N)$.
Y	Random variable defined as the time elapsing between two successfully delivered messages originating from a same node.

Let K be the number of SCs available in the selection window, i.e., in one RRI. In each RRI, each node uses one SC to broadcast its message. If more than one node uses the same SC, we assume that mixed signals cannot be separated and recovered by other nodes and thus the collision turns into a loss of the messages involved.

A node selects an idle SC[1] and persists using it for a number of times equal to its value of RC. Once RC is counted down to 0, the node decides to draw a new value of RC and persist on the same SC with probability P. With probability $1 - P$, the node switches to another idle SC and draws a new value of RC.

The reselection of a new SC is based on the measurements collected in the sensing window and results in the selection of radio resources in the selection window. We simplify this process by identifying the selection window with one RRI and assuming perfect sensing. Under these assumptions, since there are no hidden nodes, each node classifies SCs as either in use or idle, the latter state being identified only if no node is using that SC. There is no point in including SCs that are sensed as busy in the candidate SC list, since a collision would certainly be triggered. Therefore, we assume that a node that decides to jump to a new SC selects the target SC *uniformly at random among all those SCs that were idle in the previous RRI.*

The main notation used in the paper is listed in Table II.

B. Model Analysis

Let us take the point of view of one SC, referred to as the *tagged SC*. This is possible because the modeling

[1]According to the SPS algorithm, SCs eligible for selection are those that are found to be idle and those that report an RRI value of 0 in their SCI. This special value of RRI is set by a node that is using an SC for the last time, i.e., a node whose RC has dropped to 0 and that has decided not to persist on its currently used SC. We do not consider this detail, assuming that only SCs detected as idle are available for selection. Our preliminary study shows that the results obtained by the model presented in this paper do not change even if this detail is taken into account, i.e., the average AoI is minimized in both cases for a suitable value of the persistence probability.

assumptions imply full symmetry of resource use, so that all SCs are statistically equivalent. Let us define the state $X \in \{0, 1, \ldots, N\}$ associated with the SC, which is the number of nodes currently using the tagged SC for their transmission. If $X = 0$, the SC is idle and available for reservation. If $X = 1$, only a single node is using the SC, so its transmission will not collide with others. If $X > 1$, multiple nodes are using the same SC for their transmissions. Then, collision occurs and messages are lost.

Let $X_i(t)$ be the state of SC i at time t, with $i = 1, \ldots, K$ and $t \geq 0$. Let us distinguish two cases. First, if $X_i(t) > 0$, the i-th SC is currently reserved by at least one node. Thanks to sensing, no other node will attempt to jump to this SC. However, nodes currently using this SC can decide to switch to another SC, if their RC has expired. A node switches to another SC with probability

$$q = (1-c)(1-P) = \frac{1-P}{\overline{RC}}, \tag{2}$$

where $\overline{RC}$ is the average of the initial value of the RC. Then, any state $X_i(t) > 0$ can only decrease as t increases and finally reaches 0.

The second case is when $X_i(t) = 0$. Then, SC i can be selected by nodes jumping from their current SC $j \neq i$, which causes the state $X_i(t)$ to become positive.

Let us define the stochastic process $\mathbf{X}(t) = [X_1(t), \ldots, X_K(t)]$, living on the state space $\{0, 1, \ldots, N\}^K$. Thanks to the memoryless assumption on the SC reselection process, $\mathbf{X}(t)$ is a Discrete Time Markov Chain (DTMC). In view of the model assumptions, it follows that $\mathbf{X}(t)$ is time-homogeneous, irreducible, aperiodic and has a finite state space, hence it is ergodic and a unique limiting stationary probability distribution exists for the steady state process $\mathbf{X}(\infty)$. In the following, the argument ∞ will be dropped when referring to the steady-state process if there is no ambiguity.

Let the transition probability of $X_i(t)$, conditional on $\mathbf{X}_{-i}(t) = \mathbf{x}_{-i}$, be defined as

$$P_i(n,k) = \mathcal{P}(X_i(t+1) = k | X_i(t) = n, \mathbf{X}_{-i}(t) = \mathbf{x}_{-i}) \tag{3}$$

where $\mathbf{X}_{-i}(t)$ is a row vector containing all SC states $X_j(t)$ with $j \neq i$.

The conditional state transition probabilities of SC i can be written as follows:

$$\begin{cases} P_i(n,k) = \binom{n}{k}(1-q)^k q^{n-k} & \text{for } n > 0, 0 \leq k \leq n, \\ P_i(n,k) = 0 & \text{for } n > 0, k > n \\ P_i(0,k) = \binom{N}{k} w^k \left(1-w\right)^{N-k} & \text{for } n = 0, 0 \leq k \leq N, \end{cases} \tag{4}$$

where

$$\begin{cases} w = \frac{q}{1+K_e(i)} \\ K_e(i) = \sum_{j \neq i} I(X_j(t) = x_j = 0) \end{cases} \tag{5}$$

and $I(E)$ is the indicator function of the event E. Note that $K_e(i)$ is the number of idle SCs other than the considered one (SC i).

The first two equations tell us that the number of nodes using the same SC simultaneously cannot grow, thanks to channel sensing. The third equation takes into account that new nodes choose SC i when they switch from their current SC (different from i).

It is obvious that the SC states $X_i(t)$, $i = 1, \ldots, K$, are coupled together, since the number of empty SCs $K_e(i)$ is a function of the state of all SCs other than the tagged one, namely SC i. We should therefore consider the entire K-dimensional DTMC $\mathbf{X}(t) = [X_i(t), X_2(t), \ldots, X_K(t)]$, with state space size of $(N+1)^K$.

To tame the complexity of this formidable DTMC, we use a mean field approximation, which is obtained by replacing $I(X_j(t) = 0)$ with its mean, i.e., with the probability that SC j is empty, $\pi_{0,j}$. Thus, we effectively replace $K_e(i)$ (which is generally a random variable) with its mean $\overline{K}_e(i)$, namely, the mean number of idle SCs in one RRI. Quantities related to the mean field approximation are denoted by a tilde, e.g., $\tilde{X}_i(t)$ denotes the number of nodes that use SC i in the t-th RRI according to the approximate process obtained with the mean field approximation.

It can be seen that in the considered model setting, SCs are statistically equivalent, as well as nodes, so that the number of nodes transmitting on one SC has the same probability distribution for all SCs, i.e., $\tilde{X}_i(t) \sim \tilde{X}_j(t)$, $\forall i, j$. Hence, the probability distribution of $\tilde{X}_i(t)$ does not depend on the index i. Therefore, denoting the approximate transition probabilities with a tilde and dropping also index i for the sake of simpler notation, we can write

$$\begin{cases} \tilde{P}(n,k) = \binom{n}{k}(1-q)^k q^{n-k} & n > 0, 0 \leq k \leq n \\ \tilde{P}(n,k) = 0 & n > 0, k > n \\ \tilde{P}(0,k) = \binom{N}{k} \tilde{w}^k \left(1-\tilde{w}\right)^{N-k} & n = 0, 0 \leq k \leq N \end{cases} \tag{6}$$

where $\tilde{w} = q/\overline{K}_e$ and $\overline{K}_e$ is the mean number of empty SCs.

The stationary probability vector $\tilde{\pi} = [\tilde{\pi}_0, \ldots, \tilde{\pi}_N]$ is found by solving the linear system $\tilde{\pi}\tilde{\mathbf{P}} = \tilde{\pi}$, with the condition $\sum_{k=0}^{N} \tilde{\pi}_k = 1$, where $\tilde{\mathbf{P}}$ is a square matrix whose entries are $\tilde{P}(n,k)$ for $n, k = 0, 1, \ldots, N$.

The quantity $\overline{K}_e$ in Equation (6) can be expressed as follows

$$\overline{K}_e = K\tilde{\pi}_0 \tag{7}$$

From Equations (6) and (7) it is clear that the numerical solution of the DTMC $\tilde{X}(t)$ is obtained by means of a fixed-point iteration on the quantity $\tilde{\pi}_0$. For a given value of $\tilde{\pi}_0$, the one-step transition probabilities in Equation (6) are computed by using Equation (7), the DTMC stationary vector $\tilde{\pi}$ is found, and a new value of $\tilde{\pi}_0$ is found.

It is possible to exploit the special structure of the one-step transition probability matrix $\tilde{\mathbf{P}}$ to obtain a more explicit form of the fixed point equation.

It is easy to see that $\tilde{\mathbf{P}}$ has the following special structure:

$$\mathbf{P} = \begin{bmatrix} \tilde{P}(0,0) & \mathbf{v} \\ \mathbf{a} & \mathbf{A} \end{bmatrix} \tag{8}$$

where $\mathbf{v} = [\tilde{P}(0,1), \ldots, \tilde{P}(0,N)]$ is a row vector of size N, $\mathbf{a} = \mathbf{e} - \mathbf{A}\mathbf{e}$ is a column vector of size N, and $\mathbf{A}$ is a lower triangular matrix of size $N \times N$. Here $\mathbf{e}$ denotes a column vector of 1's of size N. We introduce also the notation $\mathbf{I}$ and $\mathbf{u}$ to denote the identity matrix of size $N \times N$ and a column vector of size N such that $u(k) = k$, $k = 1, \ldots, N$.

Let us split the stationary probability vector $\tilde{\pi}$ as follows: $\tilde{\pi} = [\tilde{\pi}_0, \tilde{\pi}_{-0}]$, where $\tilde{\pi}_{-0} = [\tilde{\pi}_1, \ldots, \tilde{\pi}_N]$ is a row vector of size N collecting state probabilities for states $1 \leq k \leq N$. From $\tilde{\pi}\tilde{\mathbf{P}} = \tilde{\pi}$, using Equation (8), it can be verified that

$$\tilde{\pi}_{-0} = \tilde{\pi}_0 \mathbf{v} \left(\mathbf{I} - \mathbf{A}\right)^{-1} \tag{9}$$

Then, from $\tilde{\pi}_0 + \tilde{\pi}_{-0}\mathbf{e} = 1$, we have

$$\tilde{\pi}_0 = \frac{1}{1 + \mathbf{v}\left(\mathbf{I} - \mathbf{A}\right)^{-1}\mathbf{e}} \tag{10}$$

This is a fixed point equation in $\tilde{\pi}_0$, given that the entries of $\mathbf{v}$ depend on $\tilde{w} = q/\overline{K}_e$ and hence on $\tilde{\pi}_0$ in view of Equation (7). This equation is easily handled for N and K in the range of hundreds. For very large values of N, the DTMC could be truncated, exploiting the fast decay of the probability distribution $\tilde{\pi}$.

Moreover, given the special form of entries of $\mathbf{A}$ (see Equation (6)), it is easy to check that $\mathbf{Au} = (1-q)\mathbf{u}$, i.e., $\mathbf{u}$ is a right eigenvector of $\mathbf{A}$ with eigenvalue $1-q$. For $q < 1$, it follows that

$$\sum_{k=1}^{N} k\tilde{\pi}_k = \tilde{\pi}_{-0}\mathbf{u} = \tilde{\pi}_0\mathbf{v}\left(\mathbf{I} - \mathbf{A}\right)^{-1}\mathbf{u} = \tilde{\pi}_0\mathbf{vu}\frac{1}{q} \tag{11}$$

Using expressions in Equation (6), it can be found that $\mathbf{vu} = Nq/\overline{K}_e$. Hence

$$\sum_{k=1}^{N} k\tilde{\pi}_k = \tilde{\pi}_0\frac{N}{\overline{K}_e} = \frac{N}{K} \tag{12}$$

where we have exploited Equation (7) in the last passage. This result has a simple intuitive interpretation. It expresses a conservation law, i.e., K times the mean number of nodes using one SC is just N, the overall number of nodes.

Performance metrics can be evaluated once the probability distribution $\tilde{\pi}$ is found. The average throughput in one RRI is $K\tilde{\pi}_1$, since $\tilde{\pi}$ is the probability that a node is the only one using its current SC. The success probability of a node, conditional on the node transmitting, is therefore

$$p_s = K\tilde{\pi}_1/N. \tag{13}$$

C. AoI Analysis

The time evolution of a tagged node's message delivery results can be tracked using a two-state DTMC $S(t)$, where we drop a subscript denoting the specific node, since nodes are statistically equivalent. We let $S(t) = 1$, if the tagged node's message is transmitted without collision in RRI t, otherwise we have $S(t) = 0$. The transmission of a message is successful if the selected SC is used only by the tagged node. The DTMC $S(t)$ is the basis to evaluate the average AoI of the tagged node.

The two-state Markov chain $S(t)$ captures the semi-persistent nature of the resource allocation. It shows that the semi-persistent scheduling induces a Gilbert-Elliot behavior on the communication channel of the nodes. That is, the flow of messages issued by a node alternates between success states, where each message is correctly received by the neighbors of the transmitting node, and off states, where the messages issued by the tagged node run into a series of collisions (as long as nodes persist in using the same SC) and are lost.

Given that $S(t) = 1$, the next message will be successful if (i) the node does not switch its SC, or (ii) the node switches to a new idle SC and no other node selects that same SC. Hence

$$p_{11} = \mathcal{P}(S(t+1) = 1 \,|\, S(t) = 1) = 1 - q + q\left(1 - \frac{q}{\overline{K}_1}\right)^{N-1} \tag{14}$$

Let $SC(t)$ be the subchannel where the tagged node transmits in RRI t (and is successful, since $S(t) = 1$). The quantity $\overline{K}_1$ is the mean number of idle SCs among the $K-1$ SCs other than $SC(t)$. Since the tagged node is in the "success" state, it is the only one using $SC(t)$. The other $N-1$ nodes populate the remaining $K-1$ SCs. The mean number of nodes in each busy SC other than $SC(t)$ is

$$\overline{Q}_{1,N} = \mathrm{E}[X \,|\, 1 \le X < N] = \frac{\sum_{k=1}^{N-1} k\tilde{\pi}_k}{1 - \tilde{\pi}_0 - \tilde{\pi}_N} \tag{15}$$

Then, we have

$$\overline{K}_1 = K - 1 - \frac{N-1}{\overline{Q}_{1,N}} \tag{16}$$

Using Equation (12), it can be verified that $\overline{K}_1 \approx K\pi_0$. It turns out that this approximation is within less than 1 % relative error in all of our numerical evaluations. This completes the evaluation of p_{11}.

Now we turn to the transition probability

$$p_{00} = \mathcal{P}(S(t+1) = 0 \,|\, S(t) = 0). \tag{17}$$

This is achieved by requiring that the limiting probability of state 1 coincides with the success probability, namely

$$\mathcal{P}(S(t) = 1) = \frac{1 - p_{00}}{2 - p_{11} - p_{00}} = p_s, \tag{18}$$

where p_s is given in Equation (13) and p_{11} in Equation (14).

Once we have p_{11} and p_{00} we can evaluate the moments of the time elapsing between two successful transmissions of a given node. Let Y denote the corresponding random variable, expressed in units of RRI, so that Y is an integer greater than or equal to 1. Y is defined as the time it takes a node to deliver a new successful message since when it has delivered the previous successful message. With respect to the two-state Markov chain that characterizes the node activity, this means the time to return to state $S = 1$ after having just visited state 1. If V_0 denotes the visit time in state $S = 0$, we have

$$Y = \begin{cases} 1 & \text{w.p. } p_{11}, \\ 1 + V_0 & \text{w.p. } p_{10} = 1 - p_{11}. \end{cases} \tag{19}$$

The random variable V_0 is Geometric with ratio p_{00}, hence

$$\begin{cases} \mathrm{E}[V_0] = \frac{1}{1-p_{00}} \\ \mathrm{E}[V_0^2] = \frac{1+p_{00}}{(1-p_{00})^2} \end{cases} \tag{20}$$

It follows that

$$\begin{cases} \mathrm{E}[Y] = 1 + \frac{1-p_{11}}{1-p_{00}} \\ \mathrm{E}[Y^2] = 1 + (1-p_{11})\frac{3-p_{00}}{(1-p_{00})^2} \end{cases} \tag{21}$$

By definition, we have the following final result for the average AoI and PAoI metrics

$$\begin{cases} \mathrm{E}[\mathrm{PAoI}] = \mathrm{E}[Y] \\ \mathrm{E}[\mathrm{AoI}] = \frac{\mathrm{E}[Y^2]}{2\mathrm{E}[Y]} \end{cases} \tag{22}$$

IV. Numerical Results and Discussion

In this section, we describe the simulation settings (shown in Table III) and metrics and compare the performance of the SPS algorithm for a set of N nodes sharing K SCs for three different approaches: *Proposed model* (described in Section III), MATLAB-based *Simulation model*, and *Baseline model* (inspired by the modeling approach proposed in [37]). In terms of performance metrics, we consider the transmission success probability, the PAoI, and the average AoI metrics.

Table III
MAIN SIMULATION PARAMETERS AND SETTINGS.

Parameter	Value
Number of nodes	195
Number of SCs per allocation period	200
RRI	100 ms
RC_{min}	5
RC_{max}	15

A. Simulation Model

The simulation implements the model described in Section III. It generates the RC with its standard probability distribution (uniform between RC_{min} and RC_{max}). All time quantities are normalized with respect to the duration of one RRI and are therefore expressed as multiples of the RRI.

As long as a node is the only one using an SC and messages are regularly delivered without error, its AoI will grow from zero to one RRI every RRI. If multiple nodes simultaneously decide to select an SC for subsequent use, there is a possibility that they will select the same SC, resulting in interference and failed messages. In these cases, the AoI of such nodes increases dramatically and depends on the value of the RC selected by each node. The level of AoI is critical to the safe operation of real-time safety applications and services, since nodes may not receive messages from their neighbors for a critically long time.

A visualization of the time evolution of the SC states is shown in Figure 2. Bins on the horizontal axis represent RRI times. Different rectangles on the vertical axis correspond to different SCs belonging to the same RRI period. A color code represents the number of nodes using each specific SC. White represents an empty (idle) SC, light blue represents one node occupying the SC, and dark blue represents two nodes selecting the same SC.

B. Baseline Model

The Baseline model [37] is developed to account for hidden nodes. It has no Markovian structure and neglects collisions involving more than two nodes. We cast this modeling approach into the setting considered in this paper. We then identify N_{sen} and N_r in [37] with the total number of nodes N and the number of SCs K, respectively. We replace the notation τ_{RC} in [37], which stands for the mean value of the RC, with our notation $\overline{RC}$. With this notation, the collision probability P_c is written as (see Equation (8) in [37]):

$$P_c = \frac{1}{1+P}\left[1-\left(1-\frac{1-P}{\overline{RC}N_a}\right)^{N-1}\right] \tag{23}$$

where P is the persistence probability and N_a is the mean number of available resources, i.e., the number of idle SCs in an RRI, available for reselection. According to Equation (3) in [37], we have:

$$N_a = K - N + P_c\frac{N-1}{2} \tag{24}$$

Equations (23) and (24) define a fixed point iteration on N_a. By solving numerically to find the fixed point, it is possible to evaluate the collision probability P_c and hence the PAoI as follows:

$$\mathrm{E}[\mathrm{PAoI}_{\text{Baseline}}] = \frac{1}{1-P_c} \tag{25}$$

where P_c is given in Equation (23). To be noted that the Baseline model does not describe the average AoI.

C. Result Analysis

Figure 3 shows the probability of successful transmissions as a function of the persistence probability P for the three considered approaches. Parameters values are $N = 195$, $K = 200$, the RC is uniformly distributed between 5 and 15, hence with an average value of 10.

It can be seen that both the Proposed and Baseline models are very accurate, i.e., they agree very well with the simulation results. The Proposed model is only slightly less accurate for low persistence probability values. This is due to the Geometric approximation retained in the model to draw the RC value, as opposed to the Uniform probability distribution proposed in the ETSI standard. It should be noted, however, that using the Geometric probability distribution actually *improves* performance, i.e., we can observe a higher probability of successful transmissions.

These observations are also confirmed by the performance of PAoI and AoI in the following figures. In particular, Figure 4 shows the PAoI as a function of the persistence probability P. The mean PAoI is measured in units of RRI. Again, the selection of the RC value using a Geometric distribution not only leads to an accurate estimation of the PAoI compared to simulations, but it actually decreases the obtained PAoI.

The average AoI versus P is shown in Figure 5. Similar to the previous results, replacing the RC probability distribution (Uniform, according to the standard) with a Geometric probability distribution, as done in our Proposed model, improves the AoI performance. Our model turns out to provide quite good accuracy, at least for medium to high persistence probability values.

In the following, still assuming a Geometric probability distribution for the RC, we can equivalently redefine the persistence algorithm by replacing RC and the persistence probability P by a unique parameter $q = (1-P)/\overline{RC}$ and say that the same SC is maintained with probability $1-q$ at the end of each RRI. With probability q, a new SC is selected. In other words, the persistence interval is a Geometrically distributed multiple of the RRI. As for the simulations, we set the minimum and maximum values of RC to 1, so that $\overline{RC} = 1$.

The probability of successful transmission, average PAoI and average AoI are plotted as a function of the persistence probability $P = 1-q$ in Figures 6 to 8, respectively.

Two main remarks are in order. First, the Proposed model is very accurate for all metrics considered. Second, a new qualitative behavior emerges from the analysis of AoI that has not been noticed in previous works: AoI performance is not monotonic with the persistence probability. On the contrary, an optimal value appears that corresponds to about 0.7. The intuition that explains this result is as follows. For low values of the persistence probability, nodes change their selected SC hectically, causing multiple collisions. As a result, the inter-message delivery time has a large variance, which results in a large AoI. For very high values of the persistence probability, most of the time a node is successful and delivery of update messages occurs regularly at the rate of one new message per RRI. However, once the node enters a collision state, it maintains it for a long time (high persistence). The resulting delivery process is a kind of ON-OFF communication channel,

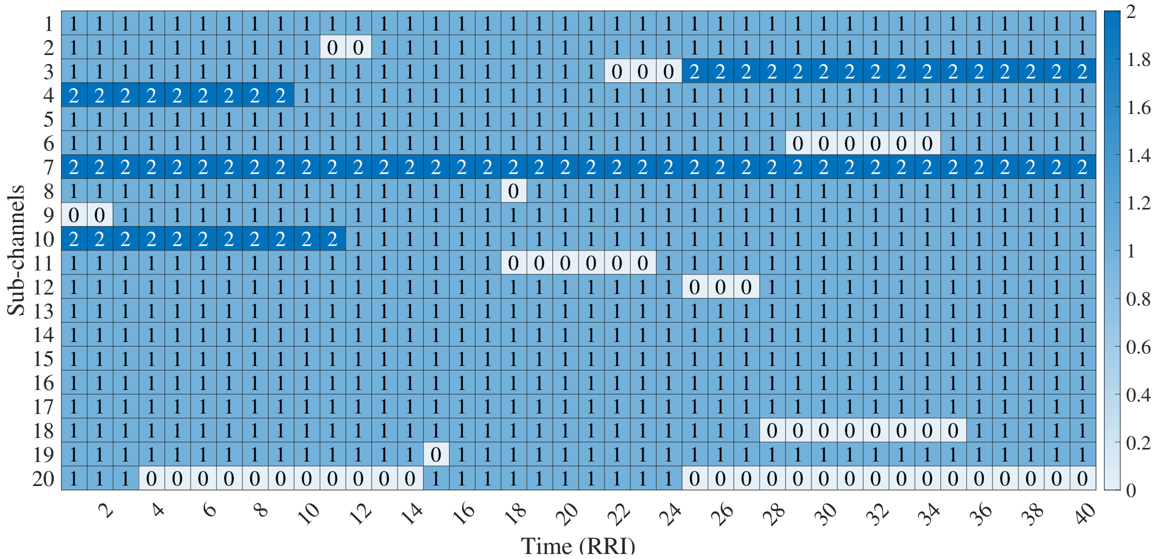

Figure 2. Example of SC state time evolution: each bin in the horizontal axis stands for an RRI time, rectangles in the vertical axis represent SCs belonging to the same RRI.

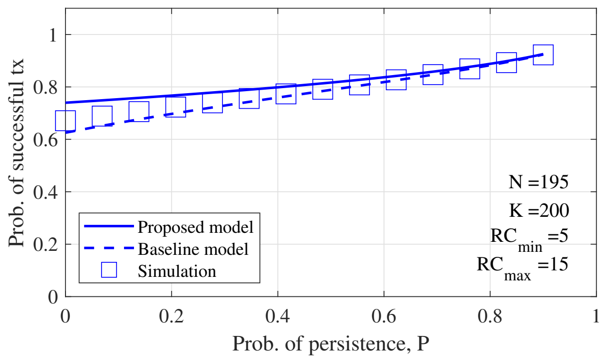

Figure 3. Probability of a successful transmission as a function of persistence probability. Analytical models versus simulation (square markers)

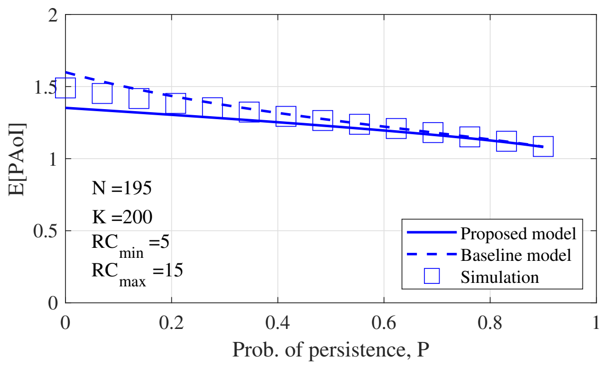

Figure 4. Average PAoI as a function of persistence probability. Analytical models versus simulation (square markers)

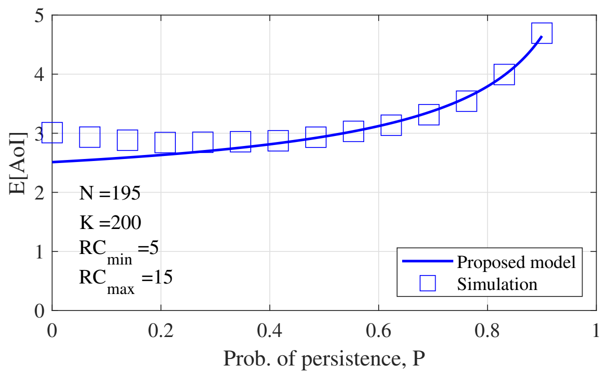

Figure 5. Average AoI as a function of persistence probability. Analytical models versus simulation (square markers)

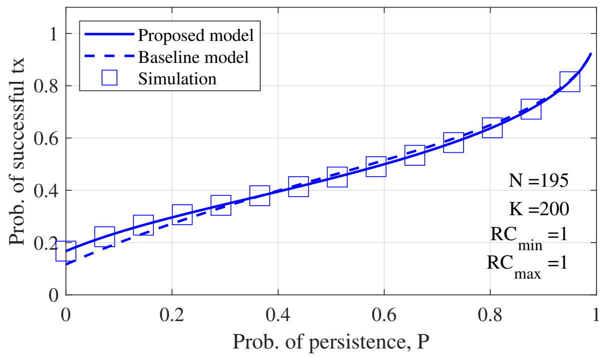

Figure 6. Probability of a successful transmission as a function of persistence probability. Analytical models versus simulation (square markers)

where long OFF times occur from time to time. While this does not affect the mean inter-message delivery time too much (hence the PAoI decreases monotonically with P), it does affect the variance of the inter-message delivery time significantly (hence the AoI increases steeply for large P).

V. Final remarks

In this paper, we have presented a study of the impact of persistence on AoI and other relevant metrics for sidelink communications, as they are currently addressed in 5G NR-V2X Mode 2 (autonomous resource selection). To this end, we presented an analytical model that has been validated through simulations. The model is based on a mean-field approximation, which is shown to provide accurate predictions. The performance metrics considered are mean AoI, PAoI, and probability of successful message delivery.

Based on the obtained performance results, we can highlight the following takeaways:

1) The proposed analytical model is accurate for all metrics considered.
2) Persistence induces a Gilbert-Elliot behavior in the

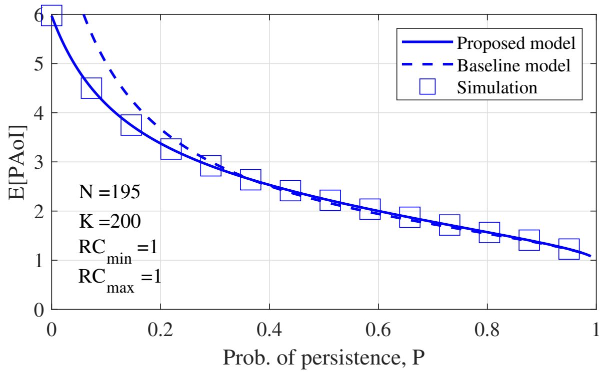

Figure 7. Average Peak AoI as a function of persistence probability. Analytical models versus simulation (square markers)

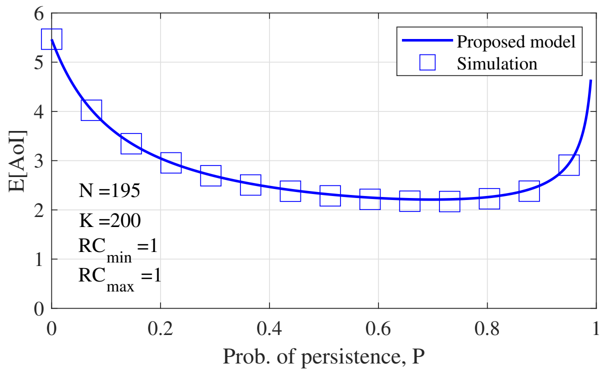

Figure 8. Average AoI as a function of persistence probability. Analytical models versus simulation (square markers)

exchange of update messages between nodes, i.e., if two or more nodes encounter a collision in selecting radio resources for their messages, the collision is repeated over time just because of persistence. On the other hand, successful message delivery is also persistent. In the end, the communication channel of a node to neighboring nodes experiences an ON-OFF behavior.

3) Replacing the probability distribution of the Reselection Counter (Uniform, according to the standard) with a Geometric probability distribution improves performance.
4) The average AoI has a non-monotonous dependence on the persistence probability P, i.e., an optimal value of the persistence probability emerges that balances the two effects that degrade the AoI: on the one hand, an excessive number of collisions in the case of frequent reselection of the subchannels used to transmit node messages, and on the other hand, an excessive persistence in a collision state, in case of high persistence levels.

To gain insight into the impact of persistence, we have addressed a rather simplified modeling framework. Next steps for this work will address more complex scenarios, where we will include larger areas, where not all nodes are within the radio range of other nodes, and also consider node mobility. In addition, other aspects of SPS that play a marginal role with respect to persistence and were therefore neglected in this study will be included in order to extend the evaluation of SPS to performance parameters and allow optimization of other parameters besides the probability of persistence.

ACKNOWLEDGEMENT

The work presented in this paper is funded by Sapienza University of Rome in the scope of "Progetti per Avvio alla Ricerca - Tipo 1", year 2022, grant assigned to the project: "Latency reduction of mode switching for modes 3 and 4 in C-V2X" (prot. AR12218167924C66). The KIT also acknowledges the support from the Helmholtz Program “Engineering Digital Futures".

REFERENCES

[1] T. Klein, T. Fenn, A. Katzenbach, H. Teigeler, S. Lins, and A. Sunyaev, “A Threat Model for Vehicular Fog Computing,” *IEEE Access*, vol. 10, pp. 133 256–133 278, 2022.

[2] M. Torrent-Moreno, J. Mittag, P. Santi, and H. Hartenstein, “Vehicle-to-vehicle communication: Fair transmit power control for safety-critical information,” *IEEE Transactions on Vehicular Technology*, vol. 58, no. 7, pp. 3684–3703, 2009.

[3] Q. Delooz et al., “Analysis and evaluation of information redundancy mitigation for v2x collective perception,” *IEEE Access*, vol. 10, pp. 47 076–47 093, 2022.

[4] H. M. Wang, S. S. Avedisov, O. Altintas, and G. Orosz, “Multi-Vehicle Conflict Management With Status and Intent Sharing Under Time Delays,” *IEEE Transactions on Intelligent Vehicles*, 2022.

[5] V. Maglogiannis, D. Naudts, S. Hadiwardoyo, D. van den Akker, J. Marquez-Barja, and I. Moerman, “Experimental V2X evaluation for C-V2X and ITS-G5 technologies in a real-life highway environment,” *IEEE Transactions on Network and Service Management*, vol. 19, no. 2, pp. 1521–1538, 2021.

[6] M. Harounabadi, D. M. Soleymani, S. Bhadauria, M. Leyh, and E. Roth-Mandutz, “V2X in 3GPP standardization: NR sidelink in release-16 and beyond,” *IEEE Communications Standards Magazine*, vol. 5, no. 1, pp. 12–21, 2021.

[7] K. Sehla, T. M. T. Nguyen, G. Pujolle, and P. B. Velloso, “Resource allocation modes in C-V2X: from LTE-V2X to 5G-V2X,” *IEEE Internet of Things Journal*, vol. 9, no. 11, pp. 8291–8314, 2022.

[8] T.-K. Liu, J. A. Silvester, and A. Polydoros, “Performance evaluation of R-ALOHA in distributed packet radio networks with hard real-time communications,” in *IEEE 45th Vehicular Technology Conference. Countdown to the Wireless Twenty-First Century*, IEEE, vol. 2, 1995, pp. 554–558.

[9] Z. Chen, N. Pappas, E. Björnson, and E. G. Larsson, “Optimizing Information Freshness in a Multiple Access Channel With Heterogeneous Devices,” *IEEE Open Journal of the Communications Society*, vol. 2, pp. 456–470, 2021.

[10] A. Baiocchi, I. Turcanu, N. Lyamin, K. Sjoöberg, and A. Vinel, “Age of Information in IEEE 802.11p,” in *17th IFIP/IEEE International Symposium on Integrated Network Management (IM): ITAVT Workshop*, Virtual Conference: IEEE, May 2021.

[11] J. Thunberg, D. Bischoff, F. A. Schiegg, T. Meuser, and A. Vinel, “Unreliable V2X Communication in Cooperative Driving: Safety Times for Emergency Braking,” *IEEE Access*, vol. 9, pp. 148 024–148 036, 2021.

[12] European Telecommunications Standards Institute, “Digital cellular telecommunications system (Phase 2+) (GSM) ; Universal Mobile Telecommunications System(UMTS) ; LTE ; 5G ; Release 16 Description; Summary of Rel-16 Work Items (3GPP TR 21.916 version 16.2.0 Release 16),” ETSI, TR 121 916 V16.2.0, Jul. 2022.

[13] M. H. C. Garcia et al., “A tutorial on 5G NR V2X communications,” *IEEE Communications Surveys & Tutorials*, vol. 23, no. 3, pp. 1972–2026, 2021.

[14] Z. Ali, S. Lagén, L. Giupponi, and R. Rouil, “3GPP NR V2X mode 2: overview, models and system-level evaluation,” *IEEE Access*, vol. 9, pp. 89 554–89 579, 2021.

[15] European Telecommunications Standards Institute, “LTE; 5G; Overall description of Radio Access Network (RAN) aspects for Vehicle-to-everything (V2X) based on LTE and NR (3GPP TR 37.985 version 17.1.1 Release 17),” ETSI, TR 137 985 V17.1.1, Apr. 2022.

[16] European Telecommunications Standards Institute, “5G; NR; Radio Resource Control (RRC); Protocol specification (3GPP TS 38.331 version 17.3.0 Release 17),” ETSI, TS 138 331 V17.3.0, Jan. 2023.

[17] M. Gonzalez-Martín, M. Sepulcre, R. Molina-Masegosa, and J. Gozalvez, “Analytical models of the performance of C-V2X mode 4 vehicular communications,” *IEEE Transactions on Vehicular Technology*, vol. 68, no. 2, pp. 1155–1166, 2018.

[18] European Telecommunications Standards Institute, “Digital cellular telecommunications system (Phase 2+) (GSM); Universal Mobile Telecommunications System (UMTS); LTE; 5G; Release description; Release 14 (3GPP TR 21.914 version 14.0.0 Release 14),” ETSI, TR 121 914 V14.0.0, Jun. 2018.

[19] M. Segata, P. Arvani, and R. L. Cigno, "A critical assessment of C-V2X resource allocation scheme for platooning applications," in *16th Annual Conference on Wireless On-demand Network Systems and Services Conference (WONS)*, IEEE, 2021, pp. 1–8.

[20] R. Molina-Masegosa, J. Gozalvez, and M. Sepulcre, "Configuration of the C-V2X mode 4 sidelink PC5 interface for vehicular communication," in *2018 14th International conference on mobile ad-hoc and sensor networks (MSN)*, IEEE, 2018, pp. 43–48.

[21] X. Gu et al., "Performance Analysis and Optimization for Semi-Persistent Scheduling in C-V2X," *IEEE Transactions on Vehicular Technology*, 2022.

[22] A. Bazzi, C. Campolo, A. Molinaro, A. O. Berthet, B. M. Masini, and A. Zanella, "On Wireless Blind Spots in the C-V2X Sidelink," *IEEE Transactions on Vehicular Technology*, vol. 69, no. 8, pp. 9239–9243, 2020.

[23] J. Wu, Y. Guo, and S. Zhou, "A Reliable Self-Adaptive Scheduling Control Protocol for Cellular V2X Mode 4," *IEEE Access*, vol. 10, pp. 63 991–64 003, 2022.

[24] L. Lusvarghi and M. L. Merani, "On the coexistence of aperiodic and periodic traffic in cellular vehicle-to-everything," *IEEE Access*, vol. 8, pp. 207 076–207 088, 2020.

[25] S. Bartoletti, B. M. Masini, V. Martinez, I. Sarris, and A. Bazzi, "Impact of the Generation Interval on the Performance of Sidelink C-V2X Autonomous Mode," *IEEE Access*, vol. 9, pp. 35 121–35 135, 2021.

[26] Y. Jeon, S. Kuk, and H. Kim, "Reducing message collisions in sensing-based semi-persistent scheduling (SPS) by using reselection lookaheads in cellular V2X," *Sensors*, vol. 18, no. 12, p. 4388, 2018.

[27] A. Haider and S.-H. Hwang, "Adaptive transmit power control algorithm for sensing-based semi-persistent scheduling in C-V2X mode 4 communication," *Electronics*, vol. 8, no. 8, p. 846, 2019.

[28] V. Todisco, S. Bartoletti, C. Campolo, A. Molinaro, A. O. Berthet, and A. Bazzi, "Performance analysis of sidelink 5G-V2X mode 2 through an open-source simulator," *IEEE Access*, vol. 9, pp. 145 648–145 661, 2021.

[29] A. Molina-Galan, B. Coll-Perales, L. Lusvarghi, J. Gozalvez, and M. L. Merani, "How does 5G NR V2X Mode 2 Handle Aperiodic Packets and Variable Packet Sizes?" In *2022 IEEE 23rd International Conference on High Performance Switching and Routing (HPSR)*, IEEE, 2022, pp. 183–188.

[30] R. D. Yates, Y. Sun, D. R. Brown, S. K. Kaul, E. Modiano, and S. Ulukus, "Age of information: An introduction and survey," *IEEE Journal on Selected Areas in Communications*, vol. 39, no. 5, pp. 1183–1210, 2021.

[31] S. Kaul, M. Gruteser, V. Rai, and J. Kenney, "Minimizing age of information in vehicular networks," in *8th Annual IEEE Communications Society Conference on Sensor, Mesh and Ad Hoc Communications and Networks*, Jun. 2011, pp. 350–358.

[32] D. Plöger, M. Segata, R. L. Cigno, and A. Timm-Giel, "Markov-modulated Models to Estimate the Age of Information in Cooperative Driving," in *2019 IEEE Vehicular Networking Conference (VNC)*, 2019, pp. 1–4.

[33] I. Turcanu, A. Baiocchi, N. Lyamin, and A. Vinel, "An Age-Of-Information Perspective on Decentralized Congestion Control in Vehicular Networks," in *19th Mediterranean Communication and Computer Networking Conference (MedComNet)*, IEEE, Jun. 2021, pp. 1–8.

[34] F. Peng, Z. Jiang, S. Zhang, and S. Xu, "Age of information optimized MAC in V2X sidelink via piggyback-based collaboration," *IEEE Transactions on Wireless Communications*, vol. 20, no. 1, pp. 607–622, 2020.

[35] A. Dayal, "Practical Algorithms and Analysis for Next-Generation Decentralized Vehicular Networks," Ph.D. dissertation, Virginia Tech, Sep. 2021.

[36] A. Fouda, R. Berry, and I. Vukovic, "Interleaved One-shot Semi-Persistent Scheduling for BSM Transmissions in C-V2X Networks," in *IEEE Vehicular Networking Conference (VNC)*, 2021, pp. 143–150.

[37] L. Cao, H. Yin, R. Wei, and L. Zhang, "Optimize Semi-Persistent Scheduling in NR-V2X: An Age-of-Information Perspective," in *2022 IEEE Wireless Communications and Networking Conference (WCNC)*, 2022, pp. 2053–2058.